Performance of Ultra-High-Performance Concrete Enhanced with Sugarcane Bagasse Ash

Yulin Wang *, Jinkang Lian, Tengfei Fu *, Said M Easa

Posted Date: 22 November 2023

doi: 10.20944/preprints202311.1443.v1

Keywords: ultra-high performance concrete； tensile-stress sensing；electrical resistivity；fractional resistance change； carbonation temperature

Article

Performance of Ultra-High-Performance Concrete Enhanced with Sugarcane Bagasse Ash

Jinkang Lian [1,2,#], Yulin Wang [1,3,*,#], Tengfei Fu [2,*], Said M. Easa [4], Yan Zhou [5] and Huawei Li [1]

[1] College of Architecture and Civil Engineering, Wuyi University, Wuyishan, Fujian 354300, China
[2] College of Transpiration and Civil Engineering, Fujian Agriculture and Forestry University, Fuzhou, Fujian 350108, China
[3] Engineering Research Center of Prevention and Control of Geological Disasters in Northern Fujian, Fujian Province University, Wuyishan, Fujian 354300
[4] Department of Civil Engineering, Toronto Metropolitan University, Toronto, Canada
[5] College of Ecology and Resource Engineering, Wuyi University, Wuyishan, Fujian 354300,China
* Correspondence: ylwanghm@163.com (Y.W.); futengfei@fafu.edu.cn (T.F.)
[#] These authors contributed equally to this work and should be considered co-first authors

Abstract; Although Sugarcane bagasse ash (SCBA) has good cementitious property, previous researchers have primarily aimed to improve the mechanical performance of conventional concrete or cement-based composites. Research is lacking on ultra-high performance concrete (UHPC), especially regarding tensile self-sensing properties. This paper aimed to comprehensively evaluate the SCBA effect on the UHPC's mechanical, electrical, and tensile self-sensing properties. The results showed that SCBA below the critical incorporation concentration (CIC) improved the UHPC's mechanical properties compared to steel fibers alone. Furthermore, adding 3.0wt% SCBA remarkably enhanced the UHPC mechanical properties where the compressive, flexural, and tensile strengths increased by 13.1%, 17.4%, and 20.6%, respectively. The SCBA content of 0.3wt% achieved the maximum UHPC electrical resistivity since values smaller or greater than this content decreased the resistivity. The SCBA-enhanced UHPC showed better tensile stress-sensing performance than UHPC without SCBA due to improved linearity and reversibility, lower hysteresis, higher sensitivity, and superior repeatability. UHPC with 0.3wt% SCBA achieved the best linearity, while UHPC with 0.9wt% SCBA showed the highest sensitivity, lowest hysteresis, and best repeatability. Overall, the content of 0.9wt% SCBA is the best in improving the overall mechanical, electrical, and tensile self-sensing performance.

Keywords: ultra-high performance concrete; tensile-stress sensing; electrical resistivity; fractional resistance change; carbonation temperature

1. Introduction

As society rapidly develops, the structural health monitoring (SHM) is becoming an essential technique for ensuring the concrete structure's health, serviceability, reliability, durability, and safety. It is also a vital approach for timely monitoring and managing accumulated damage of concrete structure [1–5]. The cement-based sensors use cement composites as conductive material. By measuring the electrical resistance to external pressure, the stress and strain states in concrete structures can be in situ monitored and evaluated in real-time [6]. Adding some functional fillers (e.g. steel fibers, and steel slag) to the concrete reduces resistivity and improves self-sensing [2–10]. This sensor is more economical and more durable than conventional sensors because it is made of cementitious materials. Therefore, functional fillers can replace cement in conventional, high-performance, self-sensing, and recycled aggregate concretes [12].

Superior mechanical properties are essential for applying self-sensing properties. The UHPC has good durability and crack resistance and therefore can be implemented for critical infrastructures. However, due to its very low electrical conductivity, UHPC alone cannot be used to achieve self-

sensing. Likewise, many researchers have used different types of conductive materials to examine the UHPC's piezoresistive sensing properties under tension. Additionally, some researchers evaluated the UHPC's feasibility for monitoring flexural performance [13–15]. Min Kyoung KIM et al. [14] showed that the UHPC as a matrix substantially improved the self-sensing performance of the steel-fiber-reinforced concrete. Furthermore, the attached electrodes showed longer polarization times than the embedded ones. Wu et al. [15] evaluated the UHPC's mechanical properties, electrical conductivity, and tensile sensitivity. During the stretching process, the resistivity of UHPC decreases first and then increases slowly as the tensile strain increases. Before the peak load, the sensitivity of UHPC to tensile strain increases as the steel fiber content increases from 1% to 2%. Doo-Yeol Yoo et al. [13] examined the tensile self-sensing of UHPC with steel fibers and CNTs. The results showed that the signal noise was minor and the resistance was much smaller in UHPFRC with CNTs because of the improved conductive pathway formation. However, nanomaterials such as CNTs and graphene cause problems such as cluster, dispersion difficulties, high cost and health risks.

Several researchers developed cement-based sensors using eco-friendly materials to overcome the drawbacks of nanomaterials. Sugarcane bagasse ash (SCBA) has potential as a supplementary cementitious material (SCM) [16,17]. Using SCBA as SCM in cementitious materials can genuinely reduce greenhouse gases and carbon footprint and address the sustainability issues of cement production [18–20]. The abundant byproduct generated from extracting juice from the sugarcane stalk is the sugarcane bagasse (SCB), making it economical as fuel for cogeneration plants [21]. For SCBA, Hernández et al. [22] stated that sugar cane straw ash, a byproduct of sugar milling, had a certain pozzolanic activity. Adding SCBA to the matrix improved the mechanical properties of cementitious materials, decreased hydration heat [23], improved concrete durability [19,24], and strengthened the cementitious matrix-aggregate interface [30]. Strategies to improve physical properties and pozzolantic activity of SCBA include calcination [25–28], sieving [29,30], grinding [29–32], and chemical treatment [33,34]. The reactive/amorphous pozzolanic oxide composition, primarily the silica content, is the critical parameter affecting the SCM's pozzolanic activity [35–41]. Therefore, SCBA may improve mechanical and durability properties of UHPC and achieve environmental and economic benefits[42]. SCBA, as a supplementary cementitious material (SCM), has been widely studied, with more than a hundred papers published [23,35], mainly focusing on conventional cement-based composites or concrete. However, research on its impact on the performance of ultra-high performance concrete (UHPC), especially UHPC's tensile self-sensing performance, is still limited.

The research aimed to comprehensively evaluate the mechanical, electrical, and self-sensing properties of SCBA-reinforced UHPC. Specifically, the study objectives are four-fold (1) to determine how the processed SCBA affects various mechanical properties of UHPC (compressive, flexural, and tensile strengths), (2) to investigate the electrical conductivity and tensile self-sensing performance of the SCBA-enhanced UHPC, and (3) to analyze the SCBA's chemical composition and porous structure and its impacts on the UHPC's mechanical property, and (4) to analyze the combined effects of SCBA and micro steel fibers on the electrical and tensile self-sensing properties using a mechanics-electricity model. Thus, this study should aid the SCBA use and promote the UHPC practical applications. The study methodology is shown in Figure 1. It involves a literature review, SCBA manufacturing process (three temperatures and five contents), UHPC fabrication, specimen preparation, tests and procedures, and results and discussion, including properties, mechanics-electricity (ME) model, and self-sensing mechanism.

Preprints (www.preprints.org) | NOT PEER-REVIEWED | Posted: 22 November 2023 doi:10.20944/preprints202311.1443.v1

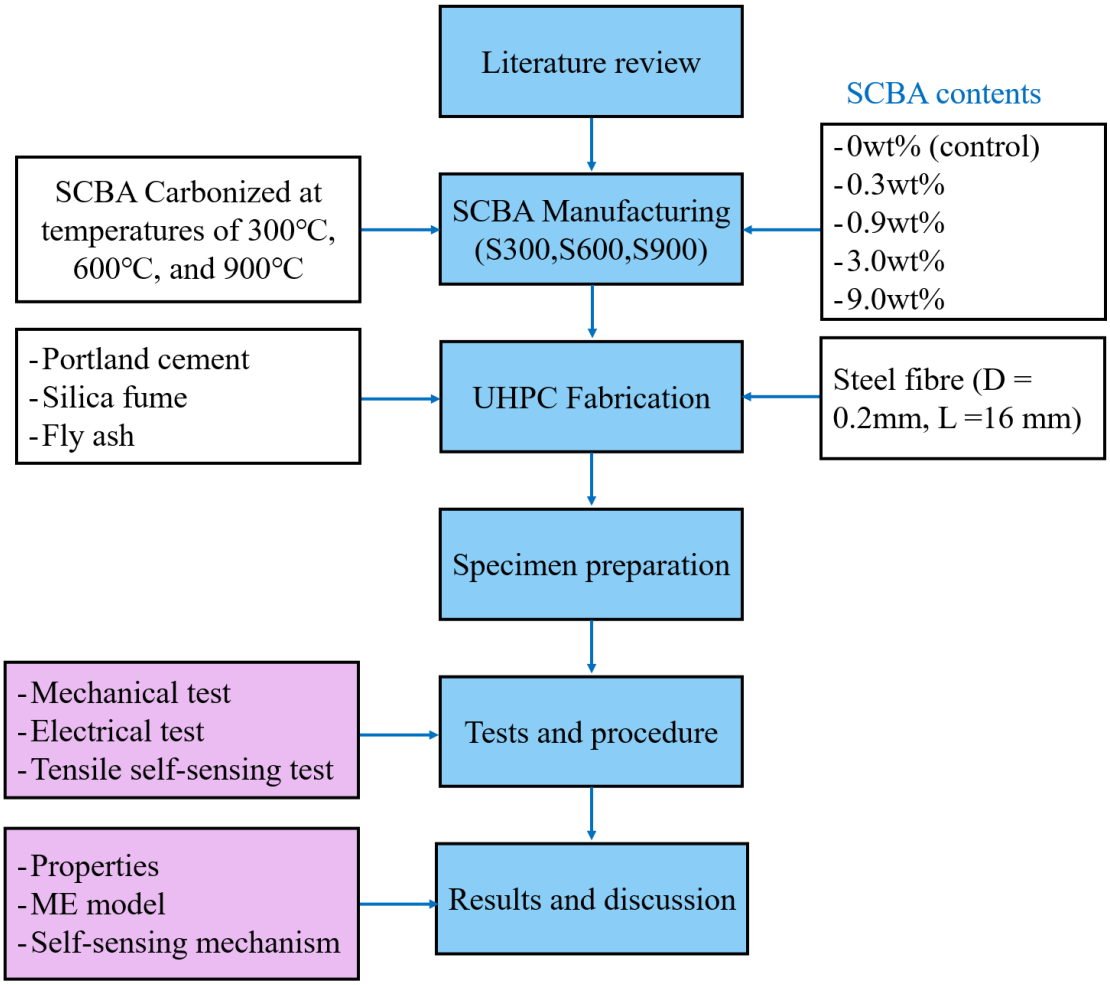

Figure 1. Study methodology.

2. Experimental Program

2.1. Manufacturing Process of SCBA

As reported in previous research findings [18], further processing of SCBA is required to improve its pozzolanic ability. This could increase (amorphous) biosilica content and fineness while decreasing impurities. It has been recommended to sieve, re-calcinate, and grind the SCBA as needed [35]. The specific process flow diagram of SCBA preparation is shown in Figure 2.

Tables 1 and 2 provide information on elemental contents, residual rate of calcinated ash and carbonation degree, and pore parameters of the porous structure of SCBA attained from different calcination temperatures. Notably, the calcination temperature significantly affects the chemical compositions and physical structure of SCBA. The chemical elements (e.g., carbon C, hydrogen H and nitrogen N), residual rate of calcinated ash, and carbonation degree decrease as the carbonation temperature increases. Among the three groups of SCBA, the sample attained at 300°C has the smallest cumulative volume and specific surface area, while possessing the largest average pore diameter (11.8 times that of SCBA achieved at 600°C). In contrast, the sample attained at 600°C has the largest cumulative volume and specific surface area (about four times and 500 times those of SCBA achieved at 300°C, respectively, while possessing the smallest average pore diameter).

The results of the liquid-nitrogen adsorption experiments in Figure 3 demonstrate that SCBA obtained at different temperatures exhibit a significant difference in pore size distribution and cumulative pore volume in size range from 0-150 nm. Furthermore, it reconfirms that SCBA attained at 300°C has the smallest cumulative volume among the three groups of SCBA, while that of SCBA achieved at 600°C is the largest.

Preprints (www.preprints.org) | NOT PEER-REVIEWED | Posted: 22 November 2023 doi:10.20944/preprints202311.1443.v1

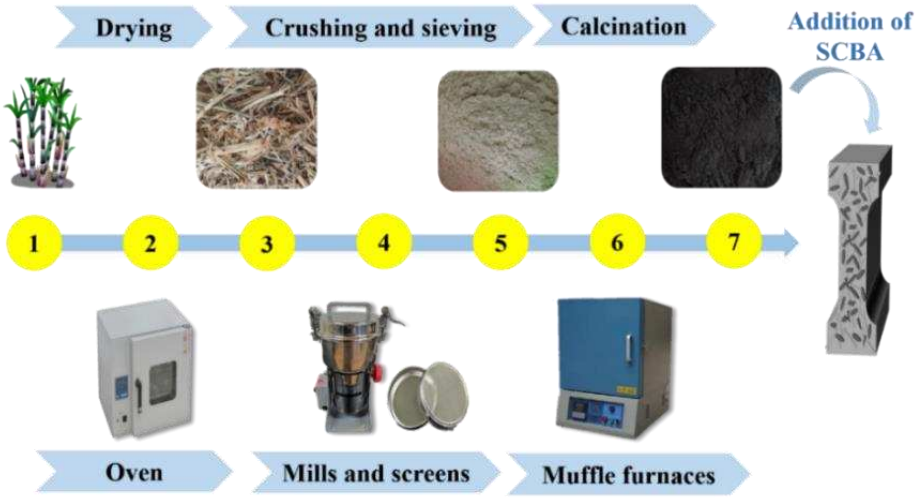

Figure 2. Process Flow Diagram of Sugarcane Bagasse Ash Preparation.

Table 1. Elemental Contents and Carbonation Degree of SCBA Affected by Carbonation Temperature.

	C,wt%	H, wt%	N, wt%	Residual Rate of Calcinated Ash, wt%	Carbonation Degree
S300	48.60	3.54	0.81	52.95	0.87
S600	38.09	1.67	0.64	40.40	0.53
S900	35.57	1.39	0.24	37.23	0.47

Note: S300、S600, and S900 refer to SCBA that was carbonized in a Muffle furnace at temperatures of 300℃, 600℃, and 900℃, respectively. C, H and N refer to the carbon, hydrogen, and nitrogen element contents, respectively.

Table 2. Parameters of Porous Structure of SCBA Attained from Different Carbonation Temperature.

	Total Pore Volume [a] (cc/g)	Average Pore Diameter [a] (nm)	Specific Surface Area (m^2/g)
S300	4.53×10^{-3}	33.64	0.54
S600	1.90×10^{-1}	2.84	267.18
S900	1.54×10^{-1}	3.02	204.54

[a] Data are for pores smaller than 150nm in diameter

Preprints (www.preprints.org) | NOT PEER-REVIEWED | Posted: 22 November 2023 doi:10.20944/preprints202311.1443.v1

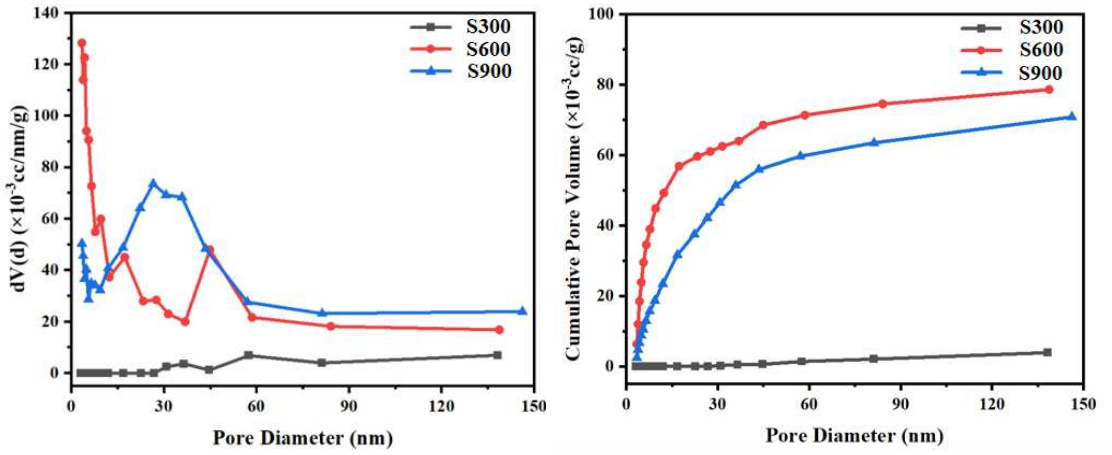

(a) (b)

Figure 3. Pore distribution curves of SCBA (carbonized at 300°C, 600°C, and 900°C): (a) primary differential curve of the cumulative pore volume and (b) cumulative Pore Volume.

2.2. Constituent Material

For UHPC fabrication, ordinary Portland cement (P.O52.5), silica fume, fly ash, and SCBA were used as binder materials, and steel fibers with a diameter of 0.2 mm and a length of 16 mm were applied as reinforcement fibers in 1.5% volume fraction of a dog-bone-shape specimen. The chemical compositions of the binder materials are shown in Table 3. As noted, all SCBAs calcined at 300°C, 600°C, and 900°C exhibit pozzolanic contents ((SiO_2+Al_2O_3+Fe_2O_3)) greater than 70%. This meets the ASTM C618 requirements of a minimum 50% and 70% for total pozzolanic content for class C pozzolans and for classes N and F pozzolans, respectively [43].

To evaluate the SCBA effect on the UHPC's mechanical properties, UHPC mixtures with three kinds of SCBAs (calcined at 300°C, 600°C, and 900°C) and four different contents (0.3wt%, 0.9wt%, 3.0wt%, and 9.0 wt% relative to the cement) were investigated. The control group was the UHPC mixture with zero SCBA. Furthermore, considering the UHPC mixtures containing a large quantity of powder and a water-to-binder (W/B) ratio of 0.2, a polycarboxylate superplasticizer (SP), in the content of 2.0wt% relative to the binders by weight, was added to all grounds of the UHPC mixtures to improve flowability. As a result, the UHPC's mix proportion is designed, as shown in Table 4.

Table 3. Chemical Compositions (in terms of oxides) of the Binder Materials (wt% by weight) [a].

Composition wt%	CaO	Al_2O_3	SiO_2	Fe_2O_3	MgO	SO3	Pozzolanic Content (SiO_2+Al_2O_3+Fe_2O_3)
Portland Cement	18.6	5.5	18.6	3.7	3.5	2.2	27.8
Silica fume	0.8	0.9	92.3	1.5	1.5	0	94.7
Fly ash	5.6	24.2	45.1	0.9	2.5	2.1	70.2
S300	4.0	10.5	57.9	1.9	3.4	2.8	70.3
S600	3.7	10.9	71.9	2.4	3.5	1.4	85.2
S900	2.9	9.8	75.2	2.1	1.9	1.4	87.1

[a] SCBA by sieving it using sieve No. 200 (75μm) for 2 min.

Preprints (www.preprints.org) | NOT PEER-REVIEWED | Posted: 22 November 2023 doi:10.20944/preprints202311.1443.v1

Table 4. Mix Proportions of UHPC (g) [a].

Mix	Cement	Silica fume	Fly ash	Water	SP	Steel fiber	SCBA
Control	1159.7	331.3	165.7	289.9	41.4	108.5	0
SCBA300	1159.7	331.3	165.7	296.0	42.3	108.5	34.8
SCBA600	1159.7	331.3	165.7	296.0	42.3	108.5	34.8
SCBA900	1159.7	331.3	165.7	296.0	42.3	108.5	34.8
SCBA0.3	1159.7	331.3	165.7	290.5	41.5	108.5	3.5
SCBA0.9	1159.7	331.3	165.7	291.7	41.7	108.5	10.4
SCBA3.0（SCBA600）	1159.7	331.3	165.7	296.0	42.3	108.5	34.8
SCBA9.0	1159.7	331.3	165.7	308.2	44.0	108.5	104.4

[a] SP = superplasticizer. SCBA0.3, SCBA0.9, SCBA3.0, and SCBA9.0 refer to concrete mixtures containing SCBA at contents of 0.3wt%, 0.9wt%, 3.0wt%, and 9.0 wt% relative to the cement, respectively, with the SCBA being obtained from calcination at a temperature of 600°C.

2.3. Specimen Preparation

The preparation processes of UHPC include blending mixtures, casting and compacting cementitious paste, and curing specimens. First, all the binder materials were dry-mixed for the 30 s in the mortar mixing pot, followd by adding and mixing the solution (water pre-mixed with superplasticizer) for 1 minute. Steel fibers were added to the paste in three batches, and the mixtures were blended at high speed for 2 min to ensure the paste was uniform. Then the paste was poured into the oiled moulds and vibrated for 1 minute on a vibrating table. After compacting the mixture, the specimens were covered with plastic film to prevent UHPC from shrinking and cracking due to moisture evaporation. The specimens were demoulded after 24 hours. The steam curing method under high temperature (90°C) was applied to the specimens for 3 days after demolding to achieve ultra-high strength rapidly. After the steam is cured, the specimens were cured at an ambient temperature of 20°C and relative humidity of 65% until testing. Figure 4 shows the specific process flow diagram of UHPC preparation.

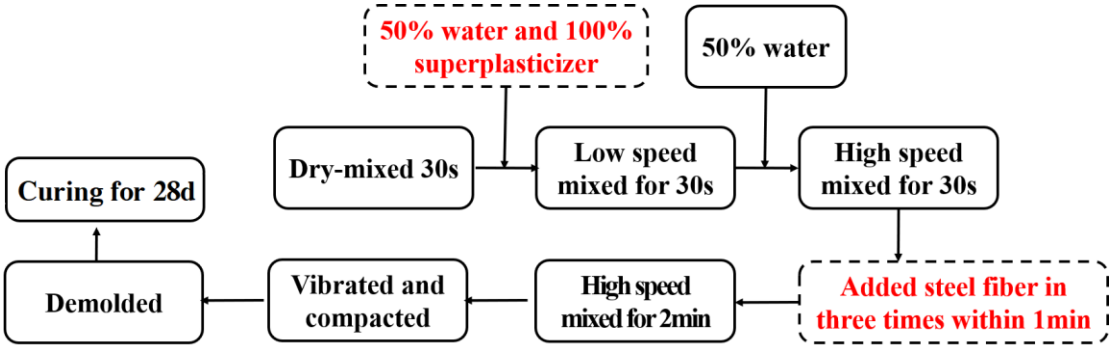

Figure 4. Process flow diagram of UHPC preparation.

2.4. Test Setup and Procedure

Mechanical Tests

The UHPC's mechanical properties were tested under uniaxial compression, flexure, and tensile forces. For the tensile strength test, direct tension was applied at the constant rate of 100 N/s on the dog-bone specimens with the geometry shown in Figure 5. For the flexural strength test, the three-

Preprints (www.preprints.org) | NOT PEER-REVIEWED | Posted: 22 November 2023 doi:10.20944/preprints202311.1443.v1

point bending load was applied at a rate of 50 N/s on the 40 mm×40 mm×160 mm specimens. The specimens were cubic for the uniaxial compression (40 mm×40 mm×40 mm).

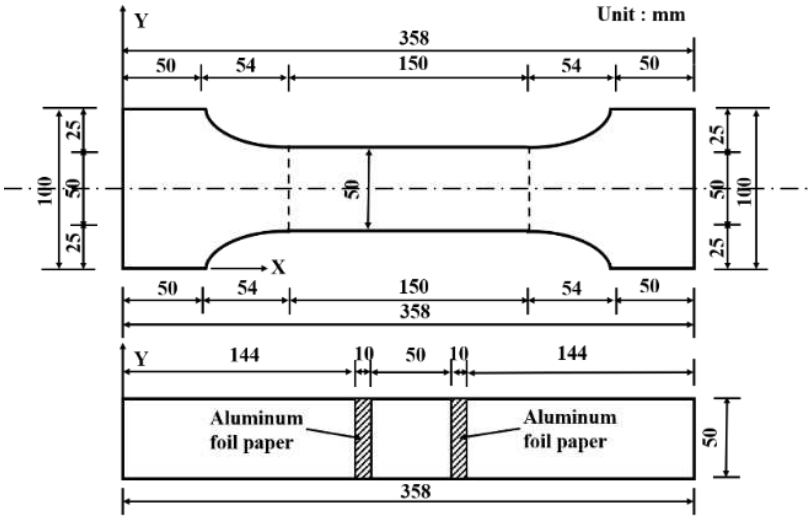

Figure 5. Geometricadetails of the dog-bone specimens.

Electrical Tests

The UHPC's electrical resistivity (ER) indicates its ability to resist transmitting ions subjected to an electrical field. The ER was measured using the two-probe method. Before measuring the specimen's ER, a layer of silver paste was first used on the specimen's surfaces to enhance electrical conductivity. Subsequently, the aluminum foil paper was attached to the silver-paste layer (Figure5). Two electrodes 50 mm apart were attached to the specimen. Alternating current (AC) was applied for approximately 10 minutes before testing to stabilize the ER of the UHPC. The ER was calculated as:

$$\rho = R \cdot \frac{A}{L} \tag{1}$$

where ρ = electrical resistivity (ER) of UHPC, R = resistance (Ω), A = specimen's cross-section area (mm^2), and L = distance between the two electrodes (mm).

Tensile Self-Sensing Tests

The tensile self-sensing properties test was conducted through two kinds of loads: single-cycle tension and multi-cyclic tension with amplitude F_{max} = 7 kN (i.e. tensile stress amplitude 2.8 MPa). First, the dog-bone-shaped specimens were stretched using a UTM at 100 N/s. In addition, an LCR meter measured the electrical resistance simultaneously as the tensile force was applied, and the response was recorded at a data frequency of 10 kHz. The fractional change of resistance (FCR) was then calculated by

$$FCR = \frac{\Delta R}{R_0} = \frac{R_X - R_0}{R_0} \tag{2}$$

where R_0 = initial resistance of the UHPC before tension application and Rx = UHPC's resistance during tension. The specimens' resistance and tensile stress were measured during loading using the data acquisition system. The self-sensing properties of UHPC under tension were evaluated (Figures 6 and 7).

To better understand the tensile self-sensing properties, the relevant parameters, (e.g., linearity, repeatability, and hysteresis error) were examined [44]. The relationship between tensile stress and the FCR of UHPC was obtained using a linear fit when a repeated load was applied. For the SCBA-UHPC, the relationship is expressed as

Preprints (www.preprints.org) | NOT PEER-REVIEWED | Posted: 22 November 2023 doi:10.20944/preprints202311.1443.v1

$$f_t = a + b\,FCR \tag{3}$$

where f_t = tensile stress and FCR = fractional change of resistance of UHPC.

The linearity (*Lin*), the offset between the tensile stress-FCR curves and the fitted regression line, is given by

$$Lin = \left(\frac{\Delta max}{\Delta FCR}\right) \times 100\% \tag{4}$$

where Δmax = maximum deviation of tensile stress-FCR curves from the fitted regression line and ΔFCR = FCR range.

The repeatability (*Rep*) is the FCR's repeat degree, given by

$$Rep = \frac{\Delta R_{max}}{\Delta FCR} \times 100\% \tag{5}$$

where ΔR_{max} = maximum repeat difference. That is, the difference of FCR for the same tensile stress in the same stroke during repeated loading.

The hysteresis (Hys) is the difference in FCR concerning the same tensile stress during cyclic variation of stress and is given by

$$Hys = \left(\frac{\Delta f_{max}}{\Delta FCR}\right) \times 100\% \tag{6}$$

where Δf_{max} = maximum difference in the measurement range.

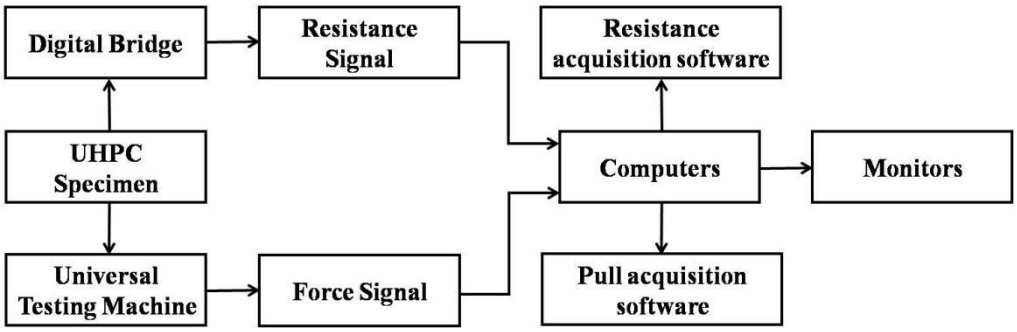

Figure 6. Data acquisition system.

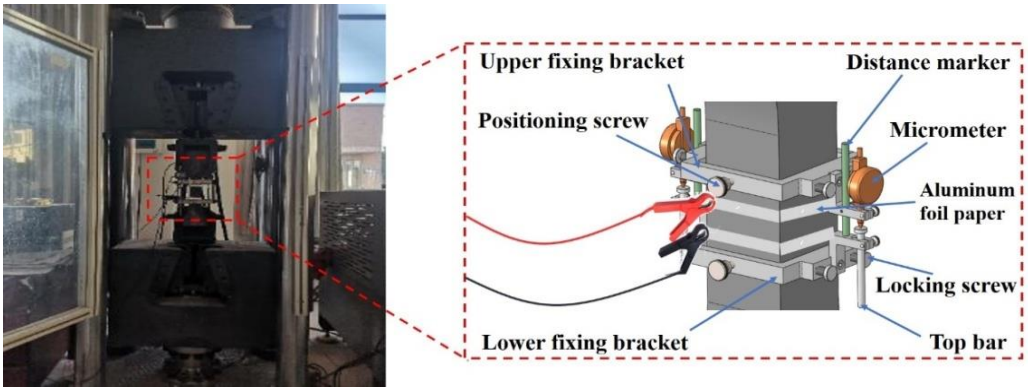

Figure 7. Tensile self-sensing Test.

3. Experimental Results and Discussion

3.1. Workability and Mechanical Properties

Table 5 shows the SCBA effect on the workability of UHPC. When the same dose (3.0wt%) was used with different calcination temperatures of SCBA, the slurry with SCBA300 had the highest

 doi:10.20944/preprints202311.1443.v1

fluidity of 212 mm and consistency of 81 mm. In contrast, the slurry with SCBA600 had the lowest fluidity of 191 mm and consistency of 44 mm, indicating the poorest workability of UHPC slurry due to the microstructure of SCBA achieved at 600°C, with a specific surface area of 267.177 m^2/g much higher than that achieved at 300°C and 900°C (Table 2). To evaluate the SCBA effect on the workability of UHPC mixtures, the SCBA calcinated at 600°C was chosen for the study with different dosing levels (0.3wt%, 0.9wt%, 3.0wt%, and 9.0wt% respectively). It was found that both the fluidity and consistency decreased as the SCBA content increased. The fluidity decreased from 209 mm to 138 mm, while the consistency decreased from 93 mm to 31 mm.

Generally, there are three main reasons for the poor workability of UHPC slurry with SCBA. Firstly, the fibrous and angular structure of the SCBA, rather than spherical particles, increases the difficulty of inflow. Secondly, the SCBA's rough surface and irregular shape increase the friction angle of the mixture, increasing the friction of motion. Finally, the SCBA's high specific surface area leads to high water absorption, thus reducing workability. It is evident that SCBA attained at 600°C calcination temperature has a much higher specific surface area than that achieved at 300°C and 900°C shown in Table 2. Therefore the UHPC slurry with SCBA600 has the worst workability for the most addition of SCBA (9.0wt%) attained at 600°C.

Table 5. Effect of SCBA on UHPC workability (mm).

	Control	**SCBA300**	**SCBA0.3**	**SCBA0.9**	**SCBA 3.0 (SCBA600)**	**SCBA9.0**	**SCBA900**
Fluidity	209	212	201	196	191	138	206
Consistency	93	81	85	58	44	31	57

The mechanical strength of SCBA with five contents of SCBA is presented in Figure 8. As noted, the compressive, flexural, and UHPC's tensile strengths initially increased and then decreased as SCBA increases. For control, SCBA0.3, SCBA0.9, SCBA3.0, and SCBA9.0, the compressive strength is 141.2, 142.7, 149.3, 159.7 and 142.0 MPa, respectively; and the flexural strengths is 23.6, 23.9, 24.6, 27.7 and 23.6 MPa, respectively; and the tensile strengths is 6.8, 6.9, 7.4, 8.2, and 7.5 Mpa, respectively. The addition of 3.0% SCBA resulted in the most remarkable improvement in UHPC's mechanical properties, with an increase in the compressive, flexural, and tensile strengths by 13.1%, 17.4%, and 20.6%, respectively, relative to that of UHPC without SCBA. However, an excessive amount of SCBA decreased the UHPC's mechanical properties, as adding 9.0wt% SCBA reduced UHPC's compressive, flexural, and tensile strengths by 11.1%, 14.8%, and 8.5%, respectively.

The main reasons for the SCBA effect on the UHPC's mechanical performance are as follows. On the one hand, SCBA acts as a pozzolanic material that has high pozzolanic activity due to the amorphous silica (SiO_2), alumina (Al_2O_3), and ferrite (Fe_2O_3), which are the principal oxides that chemically react with Portlandite calcium hydroxide during cement hydration and generate calcium silicate and aluminate hydrates. On the other hand, in the case of ground SCBA, the smaller particles contribute to the formation of additional nucleation sites for hydration products. In addition, the reduction in interface thickness leads to improved bulk density. Therefore, the enhanced UHPC's mechanical properties can be attributed to the synergistic effects of these physical changes and the volcanic ash reaction. However, incorporating an excessive amount of SCBA, precisely above 3.0%, can negatively impact the UHPC's mechanical properties. This is primarily caused by the reduced flowability and increased voids caused by the surplus SCBA within the concrete matrix.

Preprints (www.preprints.org) | NOT PEER-REVIEWED | Posted: 22 November 2023 doi:10.20944/preprints202311.1443.v1

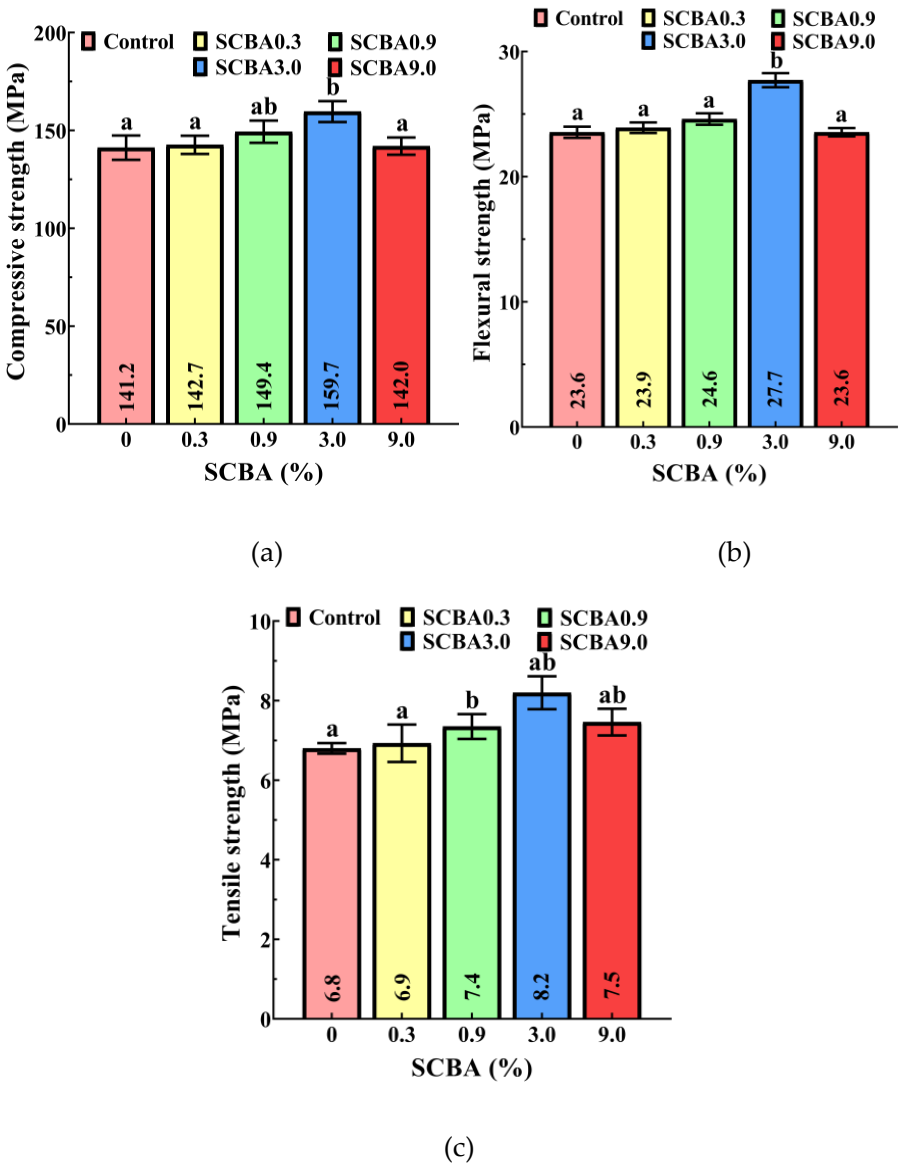

Figure 8. Effect of SCBA amounts on various mechanical properties: (a) compressive strength, (b) flexural strength, and (c) tensile strength.

3.2. Electrical Properties

Figure 9 illustrates the change in electrical resistivity of UHPC throughout 3, 14, 21, 28, and 60 days. The resistivity is affected by the curing time and decreases with increasing age due to moisture consumption during hydration. Regarding the SCBA effect, the UHPC's electrical resistivity increases as SCBA content increases for contents less than 0.3wt%. However, when the content exceeds 0.3wt%, the resistivity of UHPC decreases significantly. For example, when the curing time reaches 60 days, the resistivities of UHPC with four different dosages, measured at the frequency of 100 kHz, are 161.6, 167.3, 166.4, and 150.3 Ω·m, respectively. It is observed that there is a threshold value of SCBA for resistivity. When the additional dosage of SCBA approaches this threshold value of 0.3wt%, the largest resistivity reaches the maximum value.

The effect of SCBA on UHPC resistivity involves two aspects: on one side, chemical compositions of SCBA, such as amorphous silica and alumina, react chemically with calcium hydroxide during cement hydration and generate calcium silicate hydrates and aluminate hydrates. Consequently, the hydration products filling the gaps between conductive fillers (steel fibers and SCBA) disturb their connections, leading to higher resistivity, referred to Negative Effect (in respect of conductivity); on the other hand, adding SCBA reduces the proximity of adjacent conductive fillers

Preprints (www.preprints.org) | NOT PEER-REVIEWED | Posted: 22 November 2023 doi:10.20944/preprints202311.1443.v1

(SCBA-SCBA, steel fiber-steel fiber, and SCBA-steel fiber), and even form continuous conductive pathways in the matrix, particularly for high content of SCBA, which improves the conductivity of UHPC, herein referred to Positive Effect (in respect of conductivity). Therefore, when the dosage of SCBA is less than the threshold value (< 0.3wt%), the negative effect overwhelms the positive effect, increasing the resistivity of UHPC. Conversely, when SCBA is more than the threshold value (> 0.3wt%), the positive effect overwhelms the negative one, decreasing the UHPC resistivity.

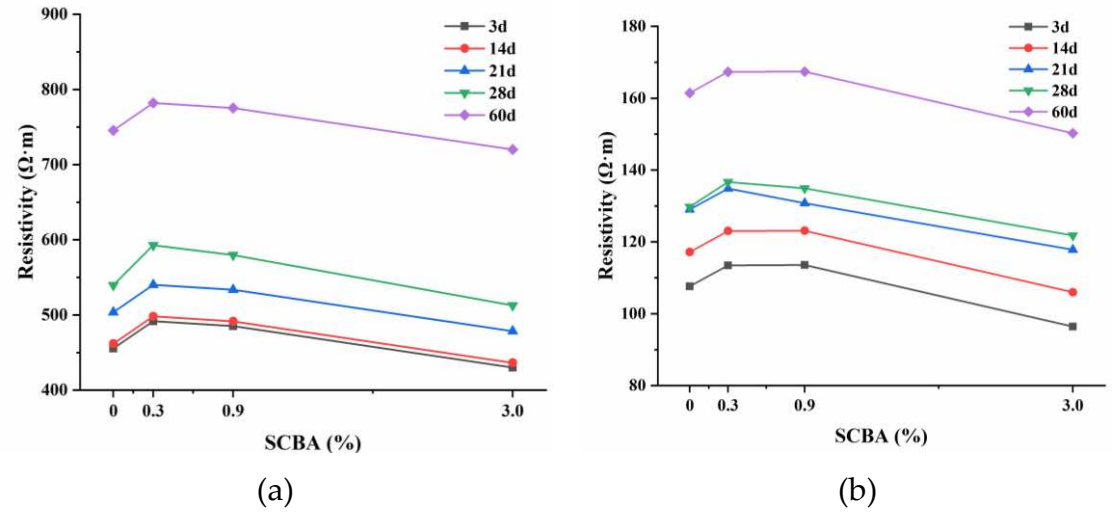

Figure 9. Electrical resistivity for UHPC with different SCBA content, tested at two frequencies: (a) 10 K Hz and (b) 100 K Hz.

3.3. Tensile Self-Sensing Properties

Single-Cyclic Tension

To evaluate the UHPC's tensile self-sensing properties, the relationship between FCR and tensile stress was established for Control, SCBA0.3, SCBA0.9, and SCBA3.0 (Figure 10), and the resulting tensile stress sensing parameters are given in Table 6. The FCR of UHPC increases monotonically with increasing tensile stress during loading and decreases monotonically with decreasing tensile stress during unloading. The curve for loading is much more linear than that for unloading, regardless of the SCBA content. However, UHPC with SCBA presents superior stress-sensing behavior compared to UHPC without SCBA regarding linearity, hysteresis, and sensitivity. Among the four mixtures, UHPC with 0.3wt% SCBA shows the best linearity, with values of 8.8% for loading and 17.0% for unloading, respectively. At the same time, UHPC with 0.9wt% SCBA exhibits the lowest hysteresis, with a value of 13.3%, much lower than that for UHPC without SCBA, which has a value of 50%.

The changes in three aspects influence UHPC self-sensing ability: tunneling effect, contact resistance, and the connection state of the conductive network due to tensile stress. Specifically, as tension increases, the proximity between adjacent conductive fillers (i.e., SCBA-SCBA, SCBA-fiber, and fiber-fiber) increases, weakening the tunneling effect and increasing the UHPC resistance. At the same time, both the conductive filler-matrix interface and the conductive filler-filler interface loosen, increasing contact resistance. Finally, when the tensile stress reaches a certain amplitude (about 2.8MPa in this study) to degrade the interfaces of the conductive fillers or cause micro-damage in the matrix, the irreversibility of resistance occurs. This is why the curve for loading is much more linear than that for unloading.

Regarding the impact of SCBA, adding SCBA reduces the distances between conductive fillers, enhancing the tunneling effect within the matrix. Thus, the resistance of UHPC with SCBA is more sensitive to changes in stress. Meanwhile, due to the presence of SCBA, the conductivity is not solely governed by steel fibers, and the UHPC maintains comparatively good conductivity even when the

Preprints (www.preprints.org) | NOT PEER-REVIEWED | Posted: 22 November 2023 doi:10.20944/preprints202311.1443.v1

steel fibers are irreversibly pulled out or micro-cracks occur in the matrix due to tensile stress (about 2.8MPa in this study). This explains the much lower hysteresis for UHPC with SCBA compared to UHPC without SCBA. However, when the additional dosage of SCBA exceeds a certain amount, continuous conductive paths will be formed in the matrix, which is irreversible if damage occurs under tension, thus changing the total current. Therefore, the hysteresis of tensile stress-sensing for UHPC with SCBA above 0.9wt% starts to worsen, although it is still better than that for UHPC without SCBA.

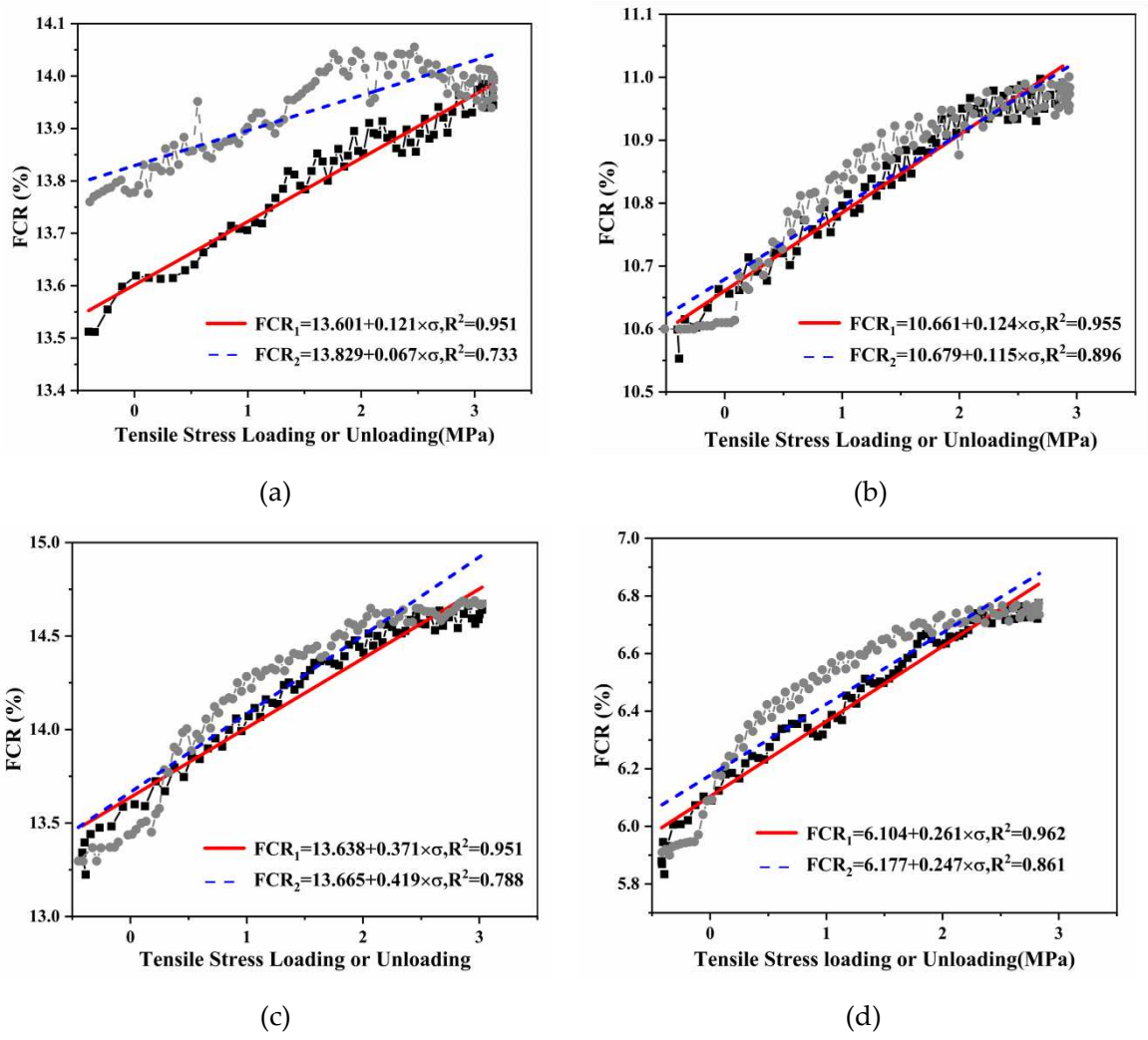

Figure 10. The relationship between FCR and tensile stress of UHPC with four different SCBA contents using the process of loading and unloading: (a) 0 wt%, (b) 0.3 wt%, (c) 0.9 wt%, and (d) 3.0 wt%. **Note:** FCR1 is tensile stress loading and FCR2 is tensile stress unloading.

Table 6. Tensile Stress-sensing Parameters of UHPC with Different Dosages of SCBA under Loading and Unloading.

sample	FCR range (%)	Linearity for loading curves (%)	Linearity for unloading curves (%)	Hysteresis (%)
Control	13.5-14.0	14.0	60.0	50.0
SCBA0.3	10.5-11.0	8.8	17.0	18.0
SCBA0.9	13.2-14.7	16.7	20.0	13.3
SCBA3.0	5.8-6.8	18.9	21.0	19.0

Preprints (www.preprints.org) | NOT PEER-REVIEWED | Posted: 22 November 2023 doi:10.20944/preprints202311.1443.v1

Multi-Cyclic Tension

The relationships between tensile stress and FCR of UHPC with four different SCBA contents (0wt%, 0.3wt%, 0.9wt%, and 3.0wt%) under the multi-cyclic tensile loads are shown in Figure 11. It is evident that the UHPC resistance increases as tensile stress increases, and decreases as tensile stress decreases in every cyclic load. Additionally, the FCR demonstrates an irreversible increase after each repeated tension, regardless of the SCBA content. However, UHPC with SCBA exhibits superior stress-sensing capabilities in the tensile stress as compared to UHPC without SCBA, due to the higher FCR amplitude (related to the sensitivity of stress sensing), higher signal-to-noise ratio, better reversibility and repeatability. As Table 7 shows, under tensile stress amplitude of 2.8MPa, the FCR amplitude is 0.25%, 0.4%, 1.45%, and 0.95% for UHPC with four different SCBA contents, respectively. This indicates that stress-sensing sensitivity first increases and then decreases with the SCBA dosage, and UHPC with 0.9wt% SCBA exhibiting the highest sensitivity. Repeatability, another important sensing parameter, is 51.6%, 10.7%, 5.3%, and 7.0% for composites with four SCBA contents, respectively, with the same trend as FCR amplitude affected by SCBA content. Among the four composites, UHPC with 0.9wt% SCBA shows the best repeatability in terms of tensile stress sensing characteristic. On the whole, doping UHPC with 0.9wt% SCBA is superior in enhancing its tensile stress self-sensing ability.

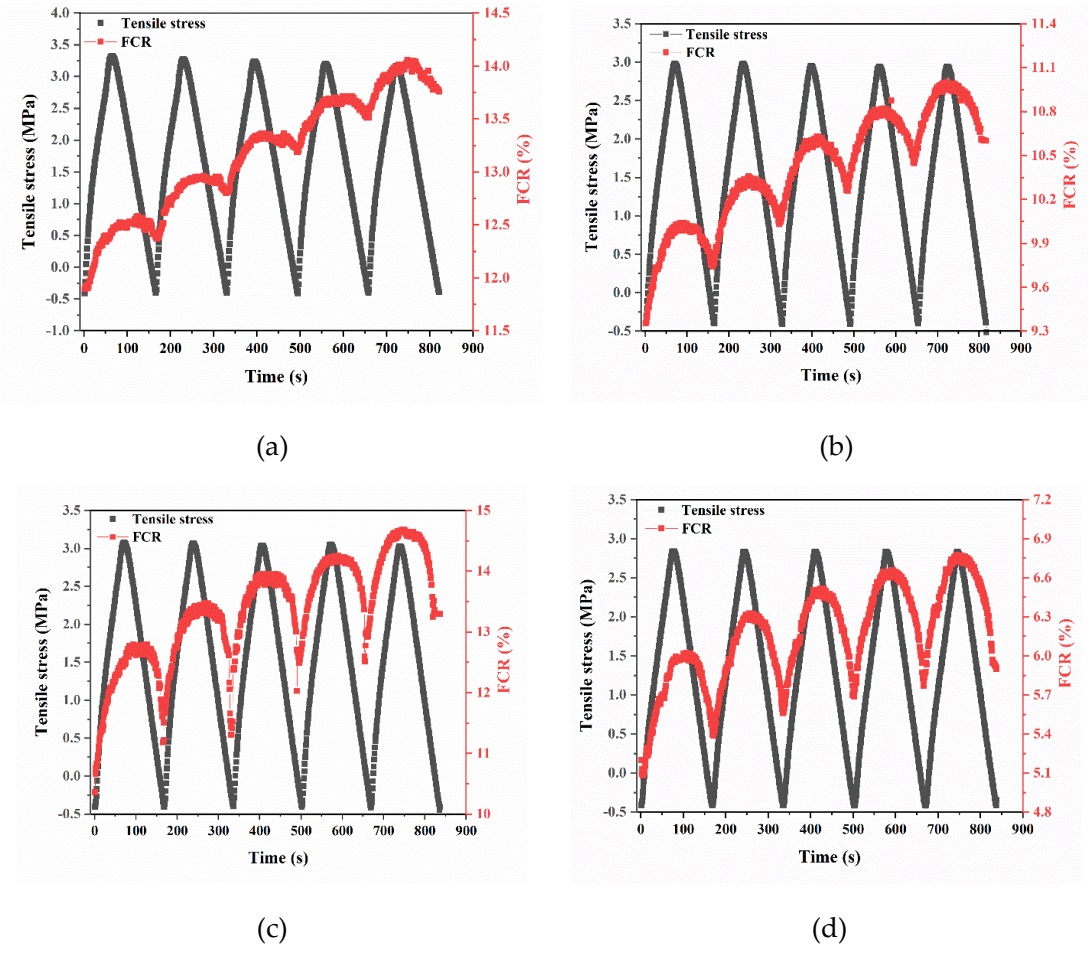

Figure 11. Cyclic tensile stress and FCR of UHPC with four different contents of SCBA: (a) 0wt%, (b) 0.3wt%, (c) 0.9wt%, and (d) 3.0wt%.

 doi:10.20944/preprints202311.1443.v1

Table 7. Tensile Stress-sensing Parameters of UHPC with Different Dosages of SCBA under Multi-Cyclic Tension.

Sample	Total FCR range (%)	Average FCR amplitude in one cycle (%)	Sensitivity (%/MPa)	Repeatability (%)
Control	11.9-14.0	0.25	0.08	51.6
SCBA0.3	9.4-11.0	0.40	0.13	10.7
SCBA0.9	10.7-14.7	1.45	0.48	5.3
SCBA3.0	5.1-6.8	0.95	0.32	7.0

4. Tensile Self-Sensing Model and Mechanism

Mechanics-Electricity Model

The mechanics-electrical models were established to analyze the mechanics-electrical relationship of the self-sensing UHPC, as shown in Figure 12. The models illustrate how the connection states of conductive fillers (steel fibers and SCBA) change under different levels of SCBA and applied tension. Adding SCBA to UHPC can reduce the proximity between conductive fillers and the potential barriers to charge migration within the UHPC matrix and even form continuous conductive channels, resulting in a decrease in UHPC resistance, which is beneficial to improve the self-sensing properties.

Self-Sensing Mechanism

The tensile stress affects UHPC resistance by changing three aspects: the gap between adjacent conductive fillers (involving tunneling effect), contact resistance, and connecting state of the electrical network. According to the electron tunneling theory, electrons within the UHPC matrix can transport between the adjacent conductive fillers, even when they are not directly connected, to generate a tunneling current, and the spacing between the conductive fillers is the crucial factor that influences the tunneling current. Therefore, application of tension on UHPC increases the gap between the adjacent conductive fillers to weaken the tunneling effect, thus increasing the UHPC resistance. At the same time, increasing the tension can reduce the tightness of not only the interface of the conductive filler and matrix but also the conductive filler-filler interface to cause the increase of electrical contact resistance, which enhances the difficulty of electrical current transportation and consequently increases the UHPC resistance.

When the additional dosage of SCBA is above a certain amount (electrical percolation value), the conductive fillers touch each other to establish a continuous electrical network, thus allowing electrical conduction occurs from one conductive filler directly to another. As regards this situation, the contribution degree of tunneling effect and interface contacts to resistance change by tension is weakened, which means the FCR of UHPC is not so vulnerable to the tensile stress, and sensing sensibility gets worse. When the tensile stress exceeds a certain amplitude to degrade the conductive filler interfaces, pull out steel fibers or cause micro damages in the matrix, which inevitably leads to the irreversibility of resistance, thus, the sensing behavior of UHPC will be irreversible.

Preprints (www.preprints.org) | NOT PEER-REVIEWED | Posted: 22 November 2023 doi:10.20944/preprints202311.1443.v1

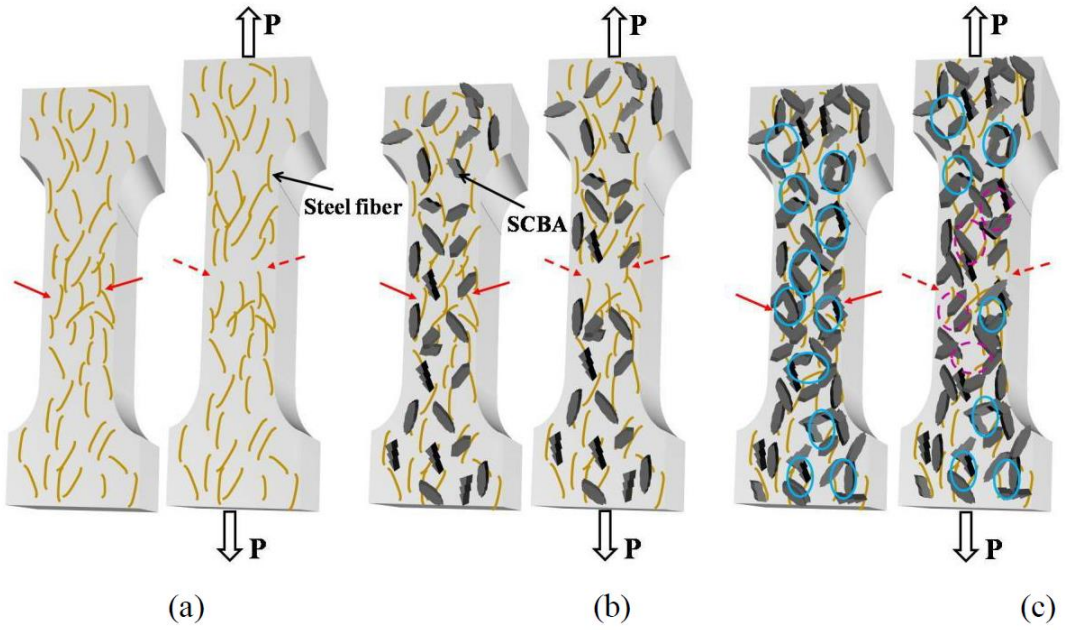

Figure 12. Mechanics-electricity Models for UHPC under tensile stress: (a) in the absence of SCBA, (b) with a certain amount of SCBA, and (c) with an excessive amount of SCBA. Note: the connection of adjacent conductive fillers, the disconnection of adjacent conductive fillers caused by tension, the formation of a continuous electrical network due to excessive SCBA addition, and the breakage of a continuous electrical network caused by tension.

5. Concluding Remarks

The SCBA is eco-friendly and low-cost, providing an excellent alternative to supplementary cementitious material (SCM). This study evaluated the mechanical, electrical, and tensile self-sensing properties of UHPC with SCBA. The SCBA's chemical composition and porous structure were investigated to analyze their influence on the mechanical property of UHPC. The impact of incorporating steel fibers and SCBA on electrical and tensile self-sensing properties was evaluated by developing and analyzing the mechanics-electricity model. Based on this study, the following conclusions comments are offered:

1. Adding processed SCBA below the critical incorporation concentration (CIC) can improve the mechanical properties of UHPC by promoting denser hydration products, such as calcium silicate and calcium aluminate hydrates. However, excessive incorporation of SCBA can reduce the workability of UHPC, suppress hydration and generate harmful voids due to redundant SCBA, ultimately leading to deterioration in the mechanical properties.
2. The incorporation of 3.0 wt% SCBA into UHPC resulted in the most significant enhancement of its compressive, flexural and tensile strength, with the improvement of 13.1%, 17.4%, and 20.6%, respectively, compared to the UHPC that only contained steel fibers without SCBA.
3. SCBA contents below 0.3wt% adversely affect the electrical resistivity of UHPC, as the hydration products disrupt the connection between conductive fillers, thereby increasing the resistivity. However, SCBA contents above 0.3wt% positively affect the electrical resistivity of UHPC as the proximity of adjacent conductive fillers decreases, or even continuous conductive pathways are formed in the matrix, resulting in reduced resistivity.
4. UHPC containing SCBA demonstrates superior tensile stress sensing properties than UHPC without SCBA, exhibiting better linearity and reversibility, lower hysteresis, higher sensitivity, and excellent repeatability. The results indicate that UHPC with 0.3wt% SCBA achieves the best linearity, while UHPC with 0.9wt% SCBA presents the highest sensitivity, lowest hysteresis, and best repeatability.

5. The relationship between FCR and tensile stress during loading is much more linear than during unloading, regardless of the SCBA content. This is due to the irreversible degradation of the interfaces between the conductive fillers or the emergence of micro-damages in the matrix during loading.
6. Overall, a content of 0.9wt% SCBA is the best in improving the overall performance of UHPC, including mechanical, electrical, and tensile self-sensing performance.

Acknowledgments: Financial support of this study is provided by: (a) the Natural Science Foundation of Fujian Province (Grant No.2022J011196, 2020J01398), (b) Wuyi University (Wuzong (2017,66), 2021XJTDKTP09, 2020-ZQGZZ-002 and 2020-SSTD-007), and (c) Innovation Experiment Project (No.202010397017).

References

1. Jing G, Siahkouhi M, Riley Edwards J, et al. Smart railway sleepers - a review of recent developments, challenges, and future prospects. *Construction and Building Materials*. 2021, 271: 121533, https://doi.org/10.1016/j.conbuildmat.2020.121533.
2. Han B G, Wang Y Y, Dong S F, et al. Smart concretes and structures: a review.*Journal of Intelligent Material System and Stuctures.* 2015,26(11):1303-1345, http://doi.org/10.1177/1045389x15586452
3. Wen S, Chung D D L. Uniaxial compression in carbon fiber reinforced cement, sensed by electrical resistivity measurement in longitudinal and transverse directions. *Cement and Concrete Research*. 2001, 31: 297-301, https://doi.org/10.1016/S0008-8846(00)00438-5.
4. Chung D D L. Damage in cement-based materials, studied by electrical resistance measurement. *Materials Science and Engineering R Reports*. 2003, 42(1): 1-40, https://doi.org/10.1016/S0927-796X(03)00037-8.
5. Wang Y L, Chung D D L. Capacitance-based defect detection and defect location determination for cement-based material. *Materials and Structures*. 2017, 50(6) : 237, https://doi.org/10.1016/S0927-796X(03)00037-8.
6. Han B G, Ding S, Yu X. Intrinsic self-sensing concrete and structures: A review. *Measurement*. 2015, 59: 110-128, https://doi.org/10.1016/j.measurement.2014.09.048.
7. Chung D D L. Self-monitoring structural materials. *Materials Science & Engineering, R-Reports*. 1998, 22(2): 57-78, https://doi.org/10.1016/S0927-796X(97)00021-1.
8. Ou J P, Baoguo H. Piezoresistive cement-based strain sensors and self-sensing concrete components. *Journal of Intelligent Material Systems and Structures*. 2009, 20(3): 329-336, https://doi.org/10.1177/1045389x08094190.
9. Banthia N, Djeridane S, Pigeon M. Electrical resistivity of carbon and steel micro-fiber reinforced cements. *Cement and Concrete Research*. 1992, 22(5): 804-814, https://doi.org/10.1016/0008-8846(92)90104-4.
10. Lee S, You I, Zi G, et al. Experimental investigation of the piezoresistive properties of cement composites with hybrid carbon fibers and nanotubes. *Sensors*. 2017, 17(11): 2516, https://doi.org/10.3390/s17112516.
11. Doo-Yeol Y, Ilhwan Y, Seung-Jung L, et al. Electrical properties of cement-based composites with carbon nanotubes, graphene, and graphite nanofibers. *Sensors*. 2017, 17(5), https://doi.org/10.3390/s17051064.
12. Chung X F A D. Self-monitoring of fatigue damage in carbon fober reinforced cement. *Cement and Concrete Research*. 1996, https://doi.org/10.1016/0008-8846(95)00184-0, https://doi.org/10.1016/0008-8846(95)00184-0.
13. Yoo D, Kim S, Lee S H. Self-sensing capability of ultra-high-performance concrete containing steel fibers and carbon nanotubes under tension. *Sensors and Actuators A: Physica*l. 2018, 276: 125-136, https://doi.org/10.1016/j.sna.2018.04.009.
14. Kim M K, Kim D J, An Y. Electro-mechanical self-sensing response of ultra-high-performance fiber-reinforced concrete in tension. *Composites Part B: Engineering*. 2018, 134: 254-264, https://doi.org/10.1016/j.compositesb.2017.09.061.
15. Wu P, Sun M Q ,Wang YJ. Study on tensile sensitivity of ultra-high performance concrete. *Bulletin of the Chinese Ceramic Society*. 2019, 38(05): 1331-1335, https://doi.org/10.16552/j.cnki.issn1001-1625.2019.05.006.
16. Torres De Sande V, Sadique M, Pineda P, et al. Potential use of sugar cane bagasse ash as sand replacement for durable concrete. *Journal of Building Engineering*. 2021, 39: 102277, https://doi.org/10.1016/j.jobe.2021.102277.
17. Ahmad W, Ahmad A, Ostrowski K A, et al. Sustainable approach of using sugarcane bagasse ash in cement-based composites: A systematic review. Case *Studies in Construction Materials*. 2021, 15: e698, https://doi.org/10.1016/j.cscm.2021.e00698.
18. Kolawole J T, Babafemi A J, Fanijo E, et al. State-of-the-art review on the use of sugarcane bagasse ash in cementitious materials. *Cement and Concrete Composites*. 2021, 118: 103975, https://doi.org/10.1016/j.cemconcomp.2021.103975.

19. Xu Q, Ji T, Gao S J, et al. Characteristics and applications of sugar cane bagasse ash waste in cementitious materials. *Materials.* 2019, 12(1): 39, https://doi.org/10.3390/ma12010039.
20. Quedou P G, Wirquin E, Bokhoree C. Sustainable concrete: potency of sugarcane bagasse ash as a cementitious material in the construction industry. *Case Studies in Construction Materials*. 2021, 14: e545, https://doi.org/10.1016/j.cscm.2021.e00545.
21. Frías M, Villar E, Savastano H. Brazilian sugar cane bagasse ashes from the cogeneration industry as active pozzolans for cement manufacture. *Cement and Concrete Composites.* 2011, 33(4): 490-496, https://doi.org/10.1016/j.cemconcomp.2011.02.003.
22. Martirena Hernandez J. F, Middendorf B, Gehrke M, et al. Use of wastes of the sugar industry as pozzolana in lime-pozzolana binders: study of the reaction. *Cement and Concrete Research*. 1998, 28(11), https://doi.org/10.1016/s0008-8846(98)00130-6.
23. Thomas B S, Yang J, Bahurudeen A, et al. Sugarcane bagasse ash as supplementary cementitious material in concrete: A review. *Materials Today Sustainability*. 2021, 15: 100086, https://doi.org/10.1016/j.mtsust.2021.100086.
24. Lima S A, Sales A, Almeida F C R, et al. Concretes made with sugarcane bagasse ash: evaluation of the durability for carbonation and abrasion tests. *Ambiente Construído*. 2011, 11(2), https://doi.org/10.1590/S1678-86212011000200014.
25. Cordeiro G C, Toledo Filho R D, Fairbairn E M R. Effect of calcination temperature on the pozzolanic activity of sugar cane bagasse ash. Construction and Building Materials. 2009, 23(10): 3301-3303, https://doi.org/10.1016/j.conbuildmat.2009.02.013.
26. Ribeiro D V, Morelli M R. Effect of calcination temperature on the pozzolanic activity of brazilian sugar cane bagasse ash (SCBA). *Materials Research*. 2014, 17(4): 974-981, http://dx.doi.org/10.1590/S1516-14392014005000093
27. Cordeiro G C, Andreão P V, Tavares L M. Pozzolanic properties of ultrafine sugar cane bagasse ash produced by controlled burning. *Heliyon*. 2019, 5(10): e2566, https://doi.org/10.1016/j.heliyon.2019.e02566.
28. Ouedraogo M, Sawadogo M, Sanou I, et al. Characterization of sugar cane bagasse ash from Burkina Faso for cleaner cement production: Influence of calcination temperature and duration. *Results in Materials*. 2022, 14: 100275, https://doi.org/10.1016/j.rinma.2022.100275.
29. Praveenkumar S, Sankarasubramanian G, Sindhu S. Strength, permeability and microstructure characterization of pulverized bagasse ash in cement mortars. *Construction and Building Materials*. 2020, 238: 117691, https://doi.org/10.1016/j.conbuildmat.2019.117691.
30. Cordeiro G C, Tavares L M, Toledo Filho R D. Improved pozzolanic activity of sugar cane bagasse ash by selective grinding and classification. *Cement and Concrete Research*. 2016, 89: 269-275, https://doi.org/10.1016/j.cemconres.2016.08.020.
31. Cordeiro G C, Toledo Filho R D, Tavares L M, et al. Ultrafine grinding of sugar cane bagasse ash for application as pozzolanic admixture in concrete. *Cement and Concrete Research*. 2009, 39(2): 110-115, https://doi.org/10.1016/j.cemconres.2008.11.005.
32. Somna R, Jaturapitakkul C, Rattanachu P, et al. Effect of ground bagasse ash on mechanical and durability properties of recycled aggregate concrete. *Materials and Design* (1980-2015). 2012, 36: 597-603, https://doi.org/10.1016/j.matdes.2011.11.065.
33. Kallioinen A, Hakola M, Riekkola T, et al. A novel alkaline oxidation pretreatment for spruce, birch and sugar cane bagasse. *Bioresource Technology.* 2013, 140: 414-420, https://doi.org/10.1016/j.biortech.2013.04.098.
34. Embong R, Shafiq N, Kusbiantoro A, et al. Effectiveness of low-concentration acid and solar drying as pre-treatment features for producing pozzolanic sugarcane bagasse ash. *Journal of Cleaner Production*. 2016, 112: 953-962, https://doi.org/10.1016/j.jclepro.2015.09.066.
35. Kolawole J T, Babafemi A J, Fanijo E, et al. State-of-the-art review on the use of sugarcane bagasse ash in cementitious materials. *Cement and Concrete Composites*. 2021, 118: 103975, https://doi.org/10.1016/j.cemconcomp.2021.103975.
36. De Soares M M N S, Garcia D C S, Figueiredo R B, et al. Comparing the pozzolanic behavior of sugar cane bagasse ash to amorphous and crystalline SiO2. *Cement and Concrete Composites*. 2016, 71: 20-25, https://doi.org/10.1016/j.cemconcomp.2016.04.005.
37. Jagadesh P, Ramachandramurthy A, Murugesan R. Evaluation of mechanical properties of Sugar Cane Bagasse Ash concrete. *Construction and Building Materials.* 2018, 176: 608-617, https://doi.org/10.1016/j.conbuildmat.2018.05.037.

38. Joshaghani A, Moeini M A. Evaluating the effects of sugar cane bagasse ash (SCBA) and nanosilica on the mechanical and durability properties of mortar. *Construction and Building Materials*. 2017, 152: 818-831, https://doi.org/10.1016/j.conbuildmat.2017.07.041.
39. Wu N S, Ji T, Huang P, et al. Use of sugar cane bagasse ash in ultra-high performance concrete (UHPC) as cement replacement. *Construction and Building Materials*. 2022, 317: 125881, https://doi.org/10.1016/j.conbuildmat.2021.125881.
40. Andrade Neto J D S, de França M J S, Amorim Júnior N S D, et al. Effects of adding sugarcane bagasse ash on the properties and durability of concrete. *Construction and Building Materials*. 2021, 266: 120959, https://doi.org/10.1016/j.conbuildmat.2020.120959.
41. Subedi S, Arce G, Hassan M, et al. Influence of production methodology on the pozzolanic activity of sugarcane bagasse ash. *Matec Web of Conferences*. 2019, 271: 7003, https://doi.org/10.1051/matecconf/201927107003.
42. Huang P, Huang B, Li J, et al. Application of sugar cane bagasse ash as filler in ultra-high performance concrete. Journal of Building Engineering, 2023, 71:106447, https://doi.org/10.1016/j.jobe.2023.106447.
43. ASTM C618, Standard specification for coal fly ash and raw or calcined natural pozzolan for use in concrete, *ASTM International, West Conshohocken*, PA, 2012, https://doi.org/10.1520/c0618.
44. Ou J P. Piezoresistive Cement-based strain sensors and self-sensing concrete components. *Journal of Intelligent Material Systems and Structures*. 2009, 20(3), https://doi.org/10.1177/1045389x08094190.